Aperture-Coupled Microstrip Open-Loop Resonators and Their Applications to the Design of Novel Microstrip Bandpass Filters

Jia-Sheng Hong, *Member, IEEE,* and Michael J. Lancaster, *Member, IEEE*

***Abstract*—The rapid growth of wireless and mobile communications has stimulated the development of multilayer filter technology. In this paper, two types of aperture-coupled microstrip open-loop resonators in a multilayer structure are proposed and investigated for the applications to the design of a new class of compact microstrip bandpass filters. The new filter configuration consists of two arrays of microstrip open-loop resonators that can be coupled through the apertures on the common ground plane. Depending on the arrangement of the apertures, different filtering characteristics can easily be realized. Electromagnetic modeling of the aperture couplings is presented. Three experimental filters of this type with Chebyshev, elliptic function, and linear phase response respectively, are described together with theoretical and experimental results. The filter asymmetric responses associated with frequency-dependent couplings are investigated.**

***Index Terms*— Microstrip filters, multilayer structure, open-loop resonators.**

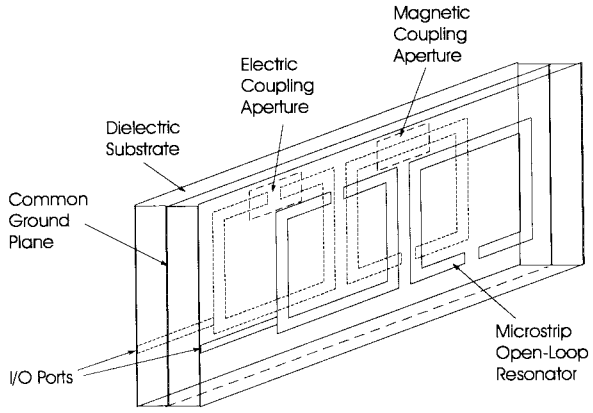

Fig. 1. Configuration of the novel microstrip bandpass filter in a multilayer configuration.

I. Introduction

BANDPASS filters are essential components in communications systems. The rapid growth of wireless and mobile communications has placed an increasing demand for new technologies to meet the challenge in meeting size, performance, and cost requirements. For this purpose, there has recently been increasing interest in multilayer bandpass filters [1]–[7]. Multilayer filter technology also provides another dimension in the flexible design and integration of other microwave components, circuits, and subsystems. The reported multilayer bandpass filters may be divided into two main categories. The first category of the multilayer bandpass filters may be composed of various coupled-line resonators that are located at different layers without any ground plane inserted between the adjacent layers, as described in [1]–[4]. In contrast, the second category of the multilayer bandpass filters utilizes aperture couplings on the common ground between the layers [5]–[6]. While the first category of the filters seems to be more suitable for wide-band applications because stronger couplings are easier to be realized, the second category of the filters would be more suitable for narrow-band applications.

The multilayer bandpass filters developed in [5] and [6] are based on the aperture-coupled dual-mode microstrip or stripline resonators and the aperture-coupled quarter-wavelength microstrip line resonators, respectively. However, it has been pointed out in [5] that the multilayered dual-mode microstrip configuration has a disadvantage as compared to the multilayered stripline in that it is more difficult to extend the concept for filters with more than four poles, while the aperture-coupled quarter-wavelength microstrip-line resonator filter requires a perfect grounding for each resonator. If the grounding is nonperfect, it can cause extra conductor losses, resulting in a lower unloaded quality factor of the resonator. Furthermore, the grounding of microstrip resonators may not be convenient for some fabrication technologies, such as the high-temperature superconducting (HTS) thin-film technology. To overcome these problems and to offer an alternative filter design, in this paper, a new class of aperture-coupled multilayer microstrip bandpass filters is introduced. The configuration of the proposed filter is shown in Fig. 1. The new filter configuration consists of two arrays of microstrip open-loop resonators that are located on the outer sides of two dielectric substrates with a common ground plane in between. Apertures on the ground plane are introduced to couple the resonators between the two resonator arrays. Depending on the arrangement of the apertures, different filtering characteristics can easily be realized.

To design the new class of filters, it requires the knowledge of mutual couplings between coupled microstrip open-loop resonators. The couplings of the open-loop resonators on the single layer of substrate have been investigated [8]. The coupling coefficients presented in [5] and [6] for aperture-coupled

Manuscript received January 1999; revised May 1999.

The authors are with the School of Electronic and Electrical Engineering, University of Birmingham, Edgbaston, Birmingham B15 2TT, U.K.

Publisher Item Identifier S 0018-9480(99)07175-6.

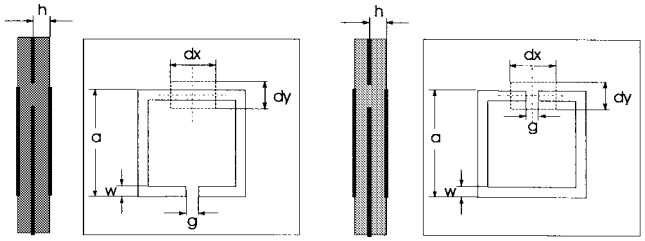

Fig. 2. Two alternative aperture couplings of back-to-back microstrip open-loop resonators. (a) Magnetic coupling. (b) Electric coupling.

dual-mode or quarter-wavelength microstrip-line resonators are not applicable for the design of the proposed filters because the couplings depend not only on the apertures, but also on the shape of resonators. Therefore, this paper will emphasize the modeling of the coupling characteristics of the aperture-coupled microstrip open-loop resonators. The theoretical models and full-wave electromagnetic (EM) simulations are presented. To demonstrate the applications of the aperture-coupled microstrip open-loop resonators, three experimental four-pole filters of this type with Chebyshev, elliptic function, and linear phase response, respectively, are described together with experimental and theoretical results. The effect of the frequency-dependent couplings on the filter responses has been investigated, and this issue will be addressed.

II. Aperture Couplings

The two types of aperture couplings that are normally encountered in the design of the proposed filters have been investigated. Fig. 2 shows the structures for the investigation, where h is the substrate thickness, a, w, and g are the dimensions of microstrip open-loop resonator, and dx and dy are the dimensions of aperture on the common ground plane. In Fig. 2(a), the aperture is centered at a position where the magnetic field is strongest for the fundamental resonant mode of the pair of microstrip open-loop resonators on both sides. Hence, the resultant coupling is the magnetic coupling and the aperture may be referred to as the magnetic aperture. In Fig. 2(b), the aperture is centered at a position where the electric field is strongest and, thus, the resultant coupling is the electric coupling and the aperture may be referred to as the electric aperture.

It has been known that the coupling coefficient of two coupled resonators may be extracted from the information of resonant-mode splitting [8]. To obtain this information, we used a full-wave EM simulator [9] to simulate the resonant frequency responses of the two aperture-coupled resonator structures of Fig. 2. Some typical simulated results are shown in Fig. 3, where the frequency axis is normalized to the resonator frequency for a zero aperture size. Two split resonant-mode frequencies are easily identified by the two resonant peaks. The larger the aperture size, the wider the separation of the two modes, indicating the stronger the coupling. However, it is noticeable that the high-mode frequency of the magnetic coupling and the low-mode frequency of the electric coupling remain unchanged regardless of the aperture size or coupling

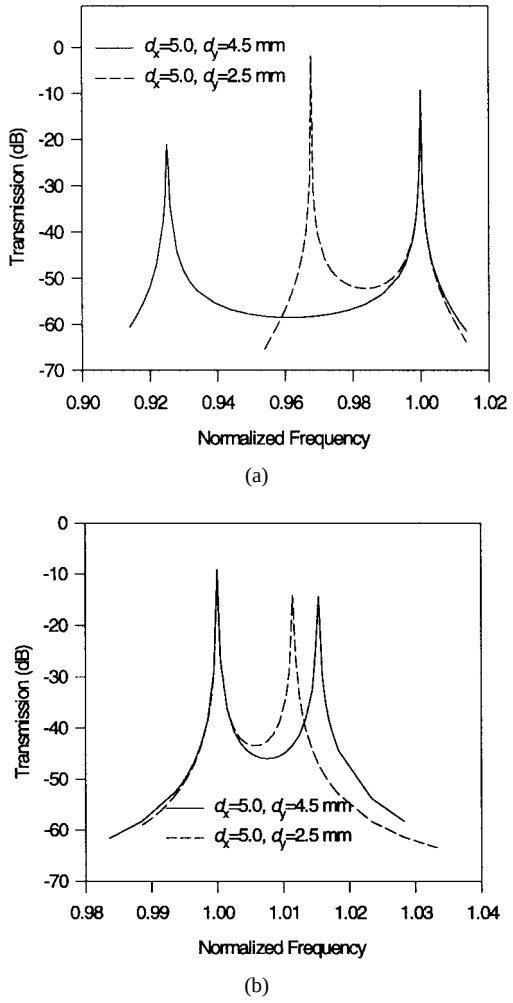

Fig. 3. Typical resonant frequency responses of aperture-coupled microstrip open-loop resonators. (a) Magnetic coupling. (b) Electric coupling.

strength. This situation is different from that observed in the coupled microstrip open-loop resonators on the single layer [8], where the two resonant-mode frequencies are always changed against coupling strength. It has been found that the difference is due to the effect of the coupling aperture on the resonant frequency of uncoupled resonators. With an aperture on the ground plane, the resonator inductance increases, whereas the resonator capacitance decreases as the aperture size is increased. Therefore, one would expect that the resonant frequency of microstrip open-loop resonators is either decreased against the magnetic aperture or increased against the electric aperture. This is verified by the full-wave EM simulation shown in Fig. 4.

In order to extract coupling coefficients of the aperture-coupled resonators, two equivalent circuits that are valid on a narrow-band basis are proposed in Fig. 5, where L and C are the self-inductance and self-capacitance, and L_m and C_m represent the mutual inductance and mutual capacitance. A notable thing is that the self-inductance in the magnetic coupling circuit is defined by $L = L_0 + L_m$, with L_0 representing the resonator inductance without the coupling aperture. On the other hand, the self-capacitance in the electric coupling circuit is defined by $C = C_0 - C_m$, with C_0

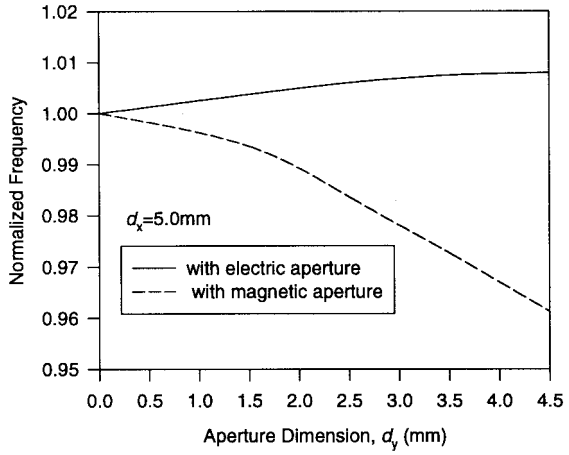

Fig. 4. Full-wave EM simulated resonant frequency of the decoupled microstrip open-loop resonators with the presence of a coupling aperture.

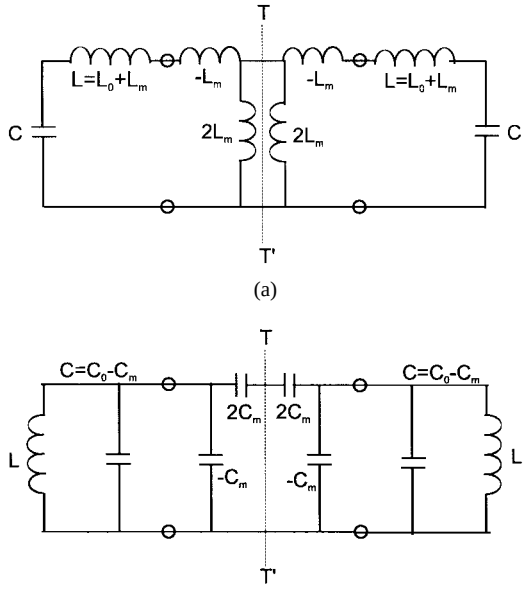

Fig. 5. Equivalent circuits for aperture-coupled microstrip open-loop resonators. (a) Magnetic coupling. (b) Electric coupling.

representing the resonator capacitance when the coupling aperture is not present. They are defined so as to account for the aperture effect. Now, if the symmetry plane T–T' in Fig. 5(a) is subsequently replaced by an electric and magnetic wall, we can obtain the following resonant-mode frequencies:

$$f_e = \frac{1}{2\pi\sqrt{L_0 C}}$$
$$f_m = \frac{1}{2\pi\sqrt{(L_0 + 2L_m)C}}. \tag{1}$$

As can be seen, the high-mode frequency f_e is independent of coupling and the low-mode frequency decreases as L_m or the coupling is increased. These two resonant frequencies correspond with those observable from the full-wave EM simulation in Fig. 3(a), and the magnetic coupling coefficient

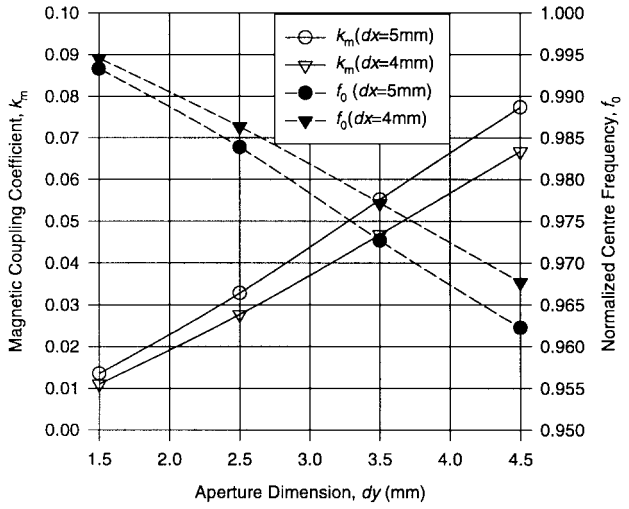

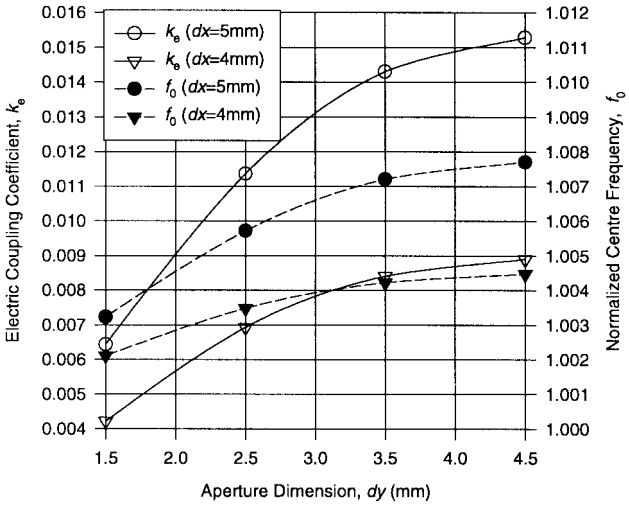

Fig. 6. Simulated coupling coefficient and normalized center frequency of aperture coupling structures in Fig. 2 with $h = 1.27$, $a = 16$, $w = 1.5$, $g = 1.0$ mm, and a substrate relative dielectric constant of 10.8. (a) With magnetic coupling aperture. (b) With electric coupling aperture.

can be extracted by

$$k_m = \frac{L_m}{L} = \frac{f_e^2 - f_m^2}{f_e^2 + f_m^2}. \tag{2}$$

Similarly, if we replace the symmetry plane T–T' in Fig. 5(b) with an electric and magnetic wall, we subsequently obtain the following resonant-mode frequencies:

$$f_e = \frac{1}{2\pi\sqrt{LC_0}}$$
$$f_m = \frac{1}{2\pi\sqrt{L(C_0 - 2C_m)}}. \tag{3}$$

In this case, the high-mode frequency f_m is increased with an increase of C_m or the coupling, while the low-mode frequency f_e is kept unchanged as what we observed in the full-wave simulation in Fig. 3(b). The electric coupling coefficient is then extracted by

$$k_e = \frac{C_m}{C} = \frac{f_m^2 - f_e^2}{f_e^2 + f_m^2}. \tag{4}$$

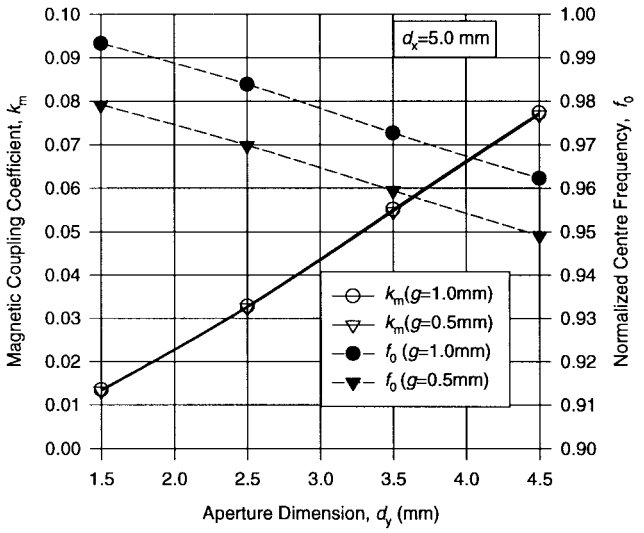

(a)

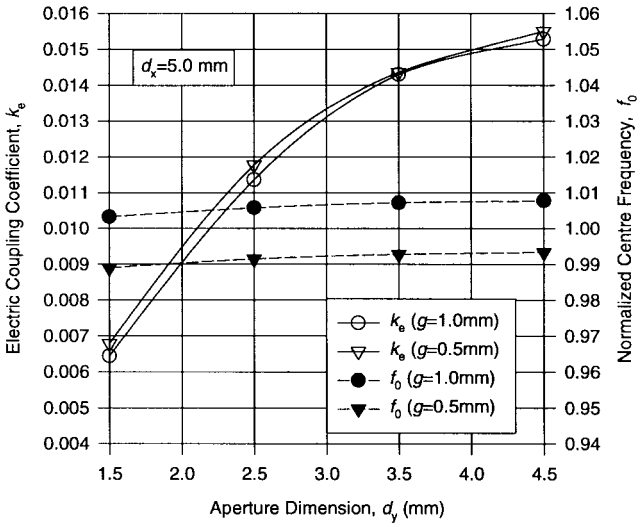

(b)

Fig. 7. Simulated open-gap effect on the coupling coefficient and normalized center frequency of aperture-coupled microstrip open-loop resonators with $h = 1.27$, $a = 16$, $w = 1.5$ mm, and a substrate relative dielectric constant of 10.8. (a) With magnetic coupling aperture. (b) With electric coupling aperture.

Fig. 6 shows some numerical results of the coupling coefficients together with the normalized center frequency of the aperture-coupled microstrip open-loop resonators. The normalized center frequency is defined as $f_0 = (f_m + f_e)/2f_r$ with f_r the resonator frequency for a zero aperture size. With the same size of the aperture, the magnetic coupling is stronger than the electric coupling. Both the couplings increase as the aperture sizes are increased. However, when the aperture sizes are increased, f_0 with the magnetic aperture decreases whereas f_0 with the electric aperture increases. This must be taken into account in the filter design. To compensate frequency shifting, we found that a more particle way is to adjust the open-gap dimension g of the open-loop resonators in Fig. 2. This is because that changing the open-gap g hardly changes the couplings, yet tunes the frequency very efficiently, as indicated by the simulated results in Fig. 7. It should be mentioned that to show the tuning effect, f_0, plotted in Fig. 7, is the frequency

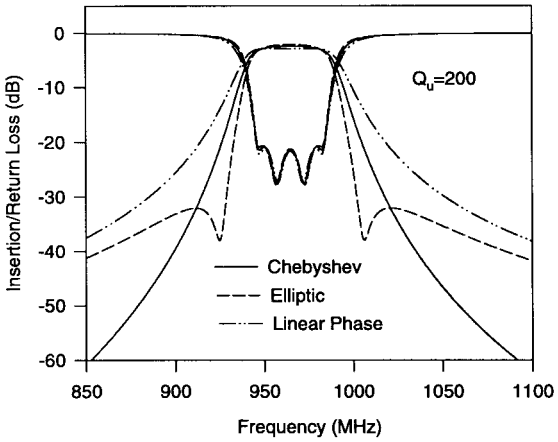

(a)

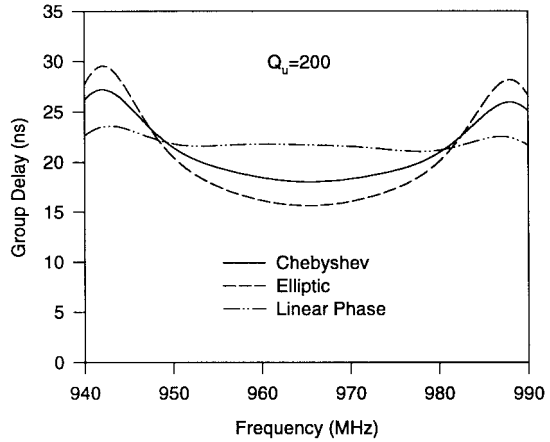

(b)

Fig. 8. Theoretical responses of experimental filters with a unloaded resonator quality factor $Q_u = 200$. (a) Insertion loss. (b) Group delay.

that normalized to a common normal frequency f_r for $g = 1.0$ mm. As can be seen when the open gap is reduced from 1.0 to 0.5 mm, the frequency shifts approximately 1.4%. This amount of frequency shifting would be more than adequate to compensate the frequency shifting due to different aperture sizes. The frequency shifting resulting from the change of g also seems quite constant over the given range of aperture sizes, and is much the same for both the magnetic and electric couplings. All this makes the frequency tuning much simpler.

III. Experimental Filters

In order to demonstrate the feasibility and capability of the proposed multilayer bandpass filters, three experimental four-pole bandpass filters having different filtering characteristics have been designed, fabricated, and tested. All the filters have a fractional bandwidth of 4.146% at a center frequency of 965 MHz. The first filter was designed to have a Chebyshev response having the following coupling matrix:

$$M_{\text{Chebyshev}} = \begin{bmatrix} 0 & 0.0378 & 0 & 0 \\ 0.0378 & 0 & 0.0290 & 0 \\ 0 & 0.0290 & 0 & 0.0378 \\ 0 & 0 & 0.0378 & 0 \end{bmatrix} \quad (5)$$

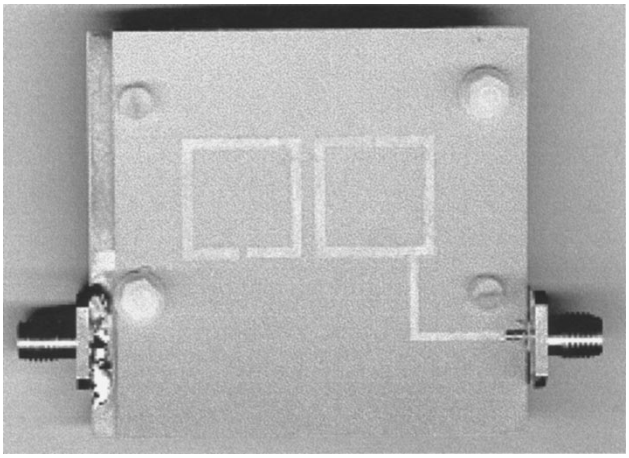

Fig. 9. Photograph of a fabricated four-pole back-to-back microstrip open-loop resonator filter.

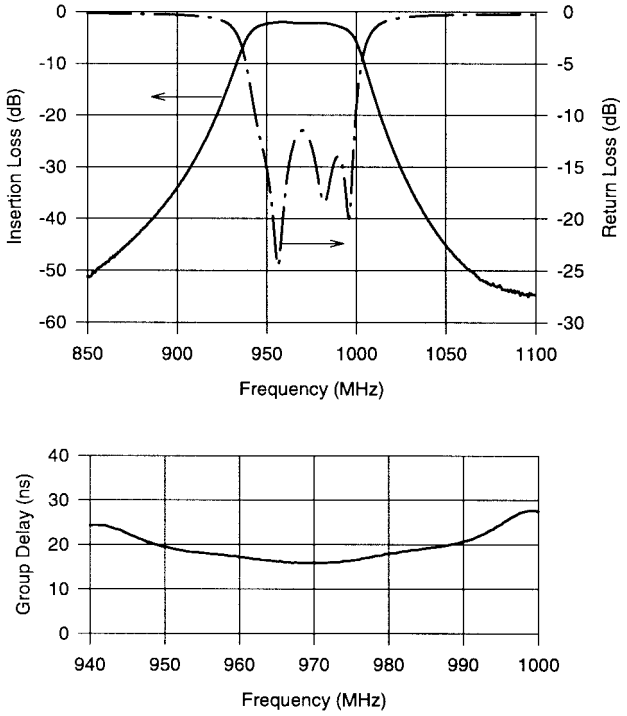

Fig. 10. Measured performance of the experimental four-pole Chebyshev filter.

and an external quality factor of 22.5045. A single magnetic aperture coupling as described above was used to realize $M_{23} = M_{32}$. The second filter was designed to have an elliptic function response having the coupling matrix

$$M_{\text{Elliptic}} = \begin{bmatrix} 0 & 0.036\,09 & 0 & -0.007\,07 \\ 0.036\,09 & 0 & 0.031\,81 & 0 \\ 0 & 0.031\,81 & 0 & 0.036\,09 \\ -0.007\,07 & 0 & 0.036\,09 & 0 \end{bmatrix} \tag{6}$$

and an external quality factor of 23.0221, in addition to a magnetic aperture coupling for $M_{23} = M_{32}$. In this case, an extra electric aperture coupling was utilized to realize $M_{14} = M_{41}$. The third filter was designed to have a linear

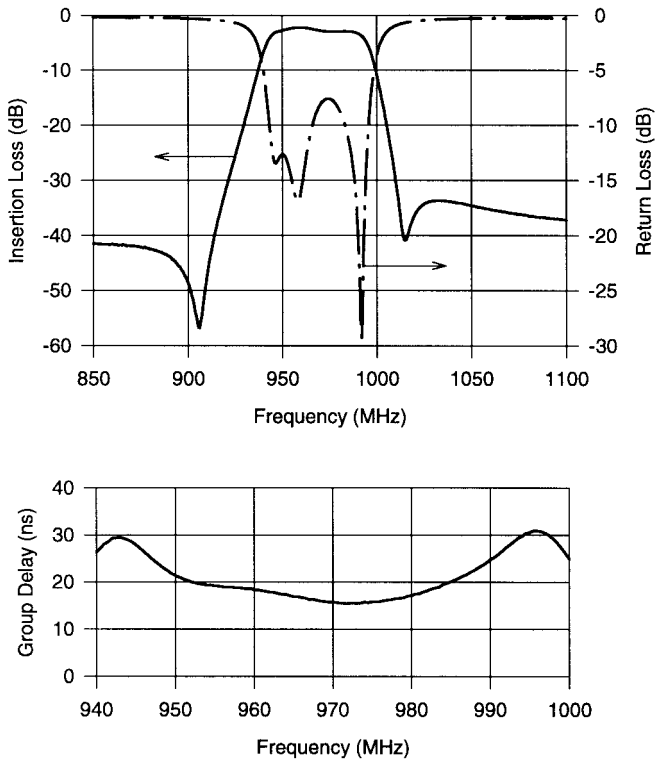

Fig. 11. Measured performance of the experimental four-pole elliptic function filter.

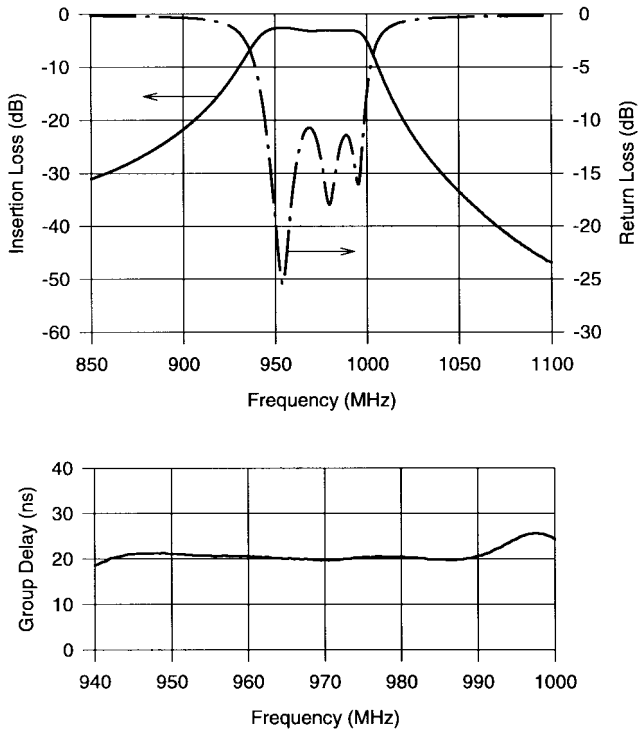

Fig. 12. Measured performance of the experimental four-pole linear phase filter.

phase response, and its coupling matrix is given by

$$M_{\text{Linear\_phase}} = \begin{bmatrix} 0 & 0.037\,76 & 0 & 0.008\,04 \\ 0.037\,76 & 0 & 0.024\,94 & 0 \\ 0 & 0.024\,94 & 0 & 0.037\,76 \\ 0.008\,04 & 0 & 0.037\,76 & 0 \end{bmatrix} \tag{7}$$

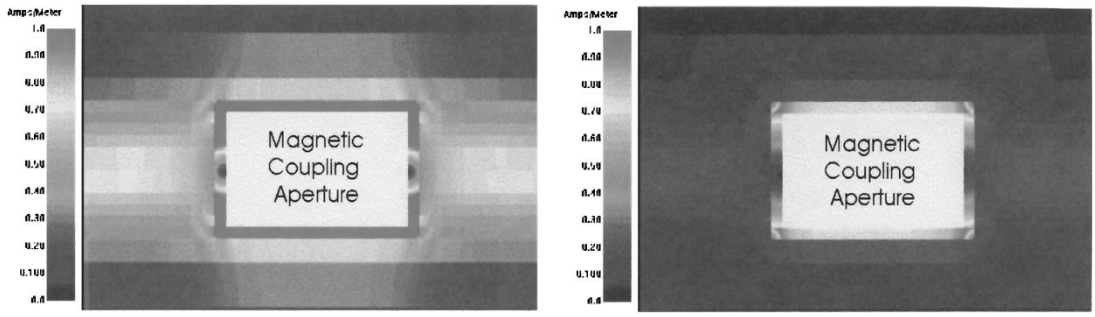

(a) (b)

Fig. 13. Magnetic-field distribution around a magnetic coupling aperture. (a) At a normalized frequency of 0.972 551. (b) At a normalized frequency of 1.027 449.

with an external quality factor of 22.5045. Note that the cross coupling $M_{14} = M_{41}$ is positive as compared with the negative one for the above elliptic function filter. Thus, both $M_{23} = M_{32}$ and $M_{14} = M_{41}$ were realized using the magnetic aperture couplings. It should be mentioned that the coupling matrices could be obtained using the synthesis method described in [10]. The theoretical responses of filters were calculated based on the coupling matrices given above. For comparison, the theoretical responses of the three experimental filters are plotted together in Fig. 8, showing distinguishable filtering characteristics that are demanded for different applications.

The filters were fabricated using copper metallization on RT/Duroid substrates with a relative dielectric constant of 10.8 and a thickness of 1.27 mm. Fig. 9 is a photograph of a four-pole experimental filter, where only two microstrip open-loop resonators on the top layer are observable. The dimensions of the resonators were $a = 16.0$ mm, $w = 1.5$ mm. It should be mentioned that except for a difference in arranging apertures in a common ground plane, the three filters have a very similar outlook. The designed Chebyshev filter used only a single magnetic aperture with a size of $dx = 4.0$ mm and $dy = 2.55$ mm. For the elliptic function filter, both magnetic and electric apertures were used, having sizes of 4.5 mm $\times$ 2.55 mm and 4.0 mm $\times$ 2.55 mm, respectively. While the linear phase filters used two magnetic apertures of 4.0 mm $\times$ 2.4 mm and 4.0 mm $\times$ 1.3 mm.

The fabricated filters were measured using an HP8510 network analyzer. The measured filter responses are plotted in Figs. 10–12. In general, good filter performance has been achieved from this single iteration of design and fabrication. In Fig. 10, the measured minimum passband insertion loss for the Chebyshev filter was approximately 2.3 dB. This loss is expected mainly due to conductor loss. The measured bandwidth was slightly wider, which would be attributed to stronger couplings. The measured elliptic function filter in Fig. 11 showed the two desirable transmission zeros. However, it exhibited an asymmetrical frequency response. This is most likely to have been caused by frequency-dependent couplings, especially the cross coupling of M_{14}. The minimum passband insertion loss for this filter was also measured to be 2.3 dB. Fig. 12 shows the measured performance of the linear phase filter. The measured minimum passband insertion loss was approximately 2.6 dB. The loss is slightly higher than that of the previous two filters, which is expected from the calculated performance in Fig. 8. The measured filter did show a linear group delay in the passband, but it also showed an asymmetrical frequency response. The latter was again attributed to the frequency-dependent couplings.

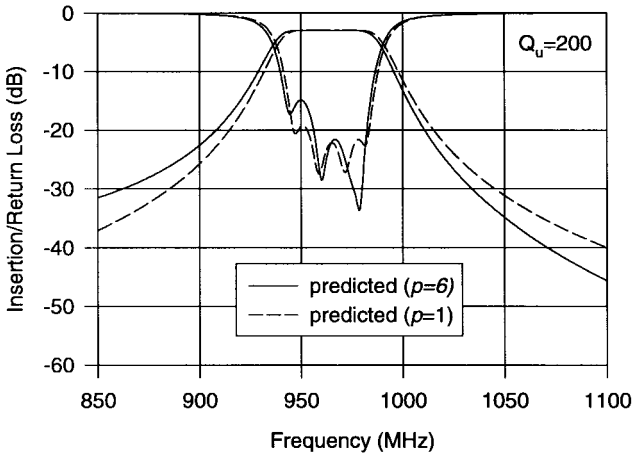

Fig. 14. Prediction of asymmetric frequency response of the linear phase filter.

IV. Frequency-Dependent Couplings

As has been mentioned above, the asymmetric frequency responses observed in the filter measurements could be attributed to the frequency-dependent couplings. To improve the filter performance, this issue must be considered. We have done some investigation and the results are presented as follows.

Fig. 13 shows the magnetic-field distribution around a magnetic coupling aperture, which was obtained using the full-wave EM simulation. The two plots in Fig. 13 were taken at the two frequencies evenly apart from the filter midband frequency, denoted by the two normalized frequencies that are normalized to the midband frequency. It can clearly be seen from the field distribution that the magnetic field is stronger at the lower frequency. Hence, it would be expected that the magnetic coupling is stronger when the frequency is lower. We might assume that the magnetic aperture coupling varies against $(f_0/f)^p$, where f_0 denotes the midband frequency and the augment p is a fitting parameter. It should be emphasized

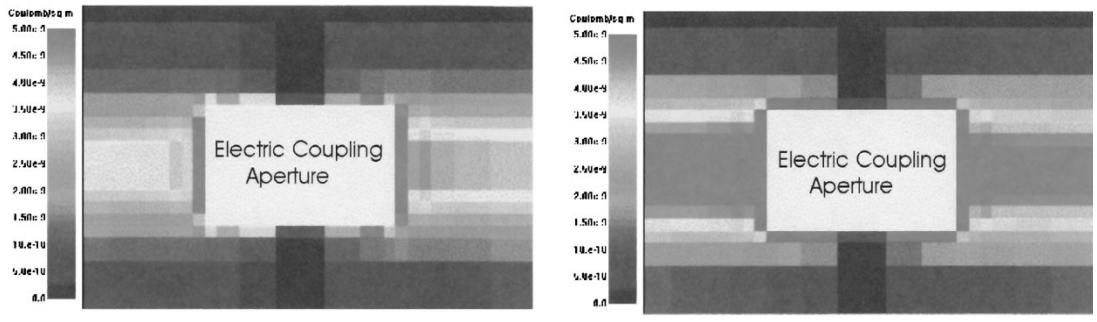

(a) (b)

Fig. 15. Electric-field distribution around an electric coupling aperture. (a) At a normalized frequency of 0.969 309. (b) At a normalized frequency of 1.030 693 1.

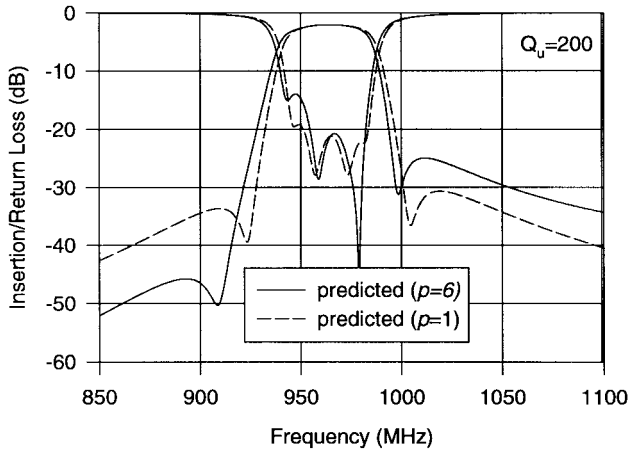

Fig. 16. Prediction of asymmetric frequency response of the elliptic function filter.

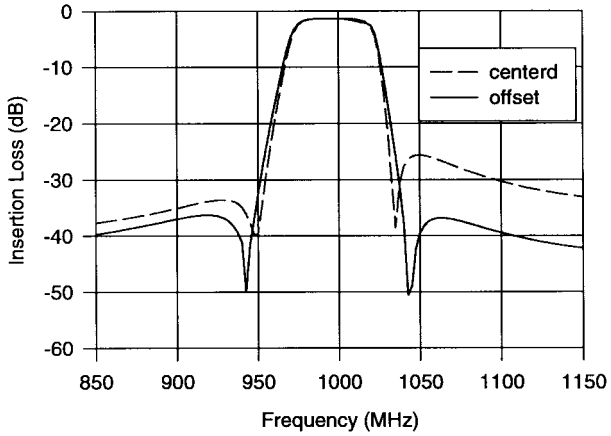

Fig. 17. Full-wave simulation of frequency response of the elliptic function filter with an offset electric aperture for the cross coupling.

that this assumed frequency-dependent coupling model is valid on a narrow-band basis. To prove this model, we carried out circuit analysis of the linear phase filter that employed two magnetic coupling apertures. The predicted response is illustrated in Fig. 14. Evidently, for $p = 6$, the predicted response is much alike to the measured one in Fig. 12.

Similarly, we simulated the electric-field distribution around an electric coupling aperture at two frequencies evenly apart from the midband frequency, and the results are shown in Fig. 15. Contrary to the magnetic distribution in Fig. 13, the electric field exhibits a stronger distribution at the higher frequency. On this ground, we would expect that the electric aperture coupling increases against frequency and, thus, we might assume that the electric coupling has a frequency dependence of $(f/f_0)^p$. This model was tested together with the above model for frequency-dependent magnetic coupling in a circuit of the experimental elliptic function filter that employed both the electric and magnetic coupling apertures. The predicted filter response is depicted in Fig. 16, showing that the asymmetric response becomes worse as the fitting parameter p is increased. As compared with the filter measurement in Fig. 11, it seems that the predicted response for $p = 6$ shows a better match of the measured one. It can also be shown that, among all couplings, the frequency-dependent cross coupling is more responsible for the asymmetric frequency response of the filter. We found that the filter asymmetric response could be much improved just by offsetting the electric coupling aperture along the open-gap arm of the microstrip open-loop resonator. This is because the electric-field distribution is not only nonuniform along the open-gap arm, but also opposite in the strength at the higher and lower rejection frequencies. Therefore, offsetting the coupling aperture in space to enhance the coupling at the lower frequency would somewhat balance the frequency-dependent coupling. This approach was confirmed by the full-wave simulation of a modified elliptic function filter having an offset electric aperture of 4.0 mm $\times$ 1.5 mm with 0.5-mm offset in the x-direction. The simulated results are shown in Fig. 17, demonstrating a much more symmetric frequency response of the modified filter.

V. Conclusion

We have presented the investigation of two types of aperture-coupled microstrip open-loop resonators in a multilayer configuration. These two coupling structures are essential components for a new class of compact microstrip bandpass filters. The theory and method for extracting the coupling coefficients for filter design have been developed. The full-wave EM modeling of the aperture couplings has been described. Depending on the arrangement of the apertures,

different filtering characteristics can easily be realized by the proposed filters. For demonstration, three four-pole bandpass filters of this type with Chebyshev, elliptic function, and linear phase responses, respectively, have been designed, fabricated, and tested. The measured results together with the theoretical ones have been presented. The issue of frequency-dependent couplings has been addressed. It has been shown that the new class of filters hold promise for wireless and mobile communications applications. The new filter configuration is also attractive for HTS thin-film implementation.

REFERENCES

[1] W. Schwab and W. Menzel, "Compact bandpass filters with improved stop-band characteristics using planar multilayer structures," in *IEEE MTT-S Symp. Dig.*, 1992, pp. 1207–1210.

[2] C. Person, A. Sheta, J. P. Coupez, and S. Toutain, "Design of high performance bandpass filters by using multilayer thick-film technology," in *Proc. 24th European Microwave Conf.*, Cannes, France, 1994, pp. 466–471.

[3] W. Schwab, F. Boegelsack, and W. Menzel, "Multilayer suspended stripline and coplanar line filters," *IEEE Trans. Microwave Theory Tech.*, vol. 42, pp. 1403–1406, July 1994.

[4] C. Cho and K. C. Gupta, "Design methodology for multilayer coupled line filters," in *IEEE MTT-S Symp. Dig.*, June 1997, pp. 785–788.

[5] J. A. Curtis and S. J. Fiedzuszko, "Multilayered planar filters based on aperture coupled, dual mode microstrip or stripline resonators," in *IEEE MTT-S Symp. Dig.*, 1992, pp. 1203–1206.

[6] S. J. Yao, R. R. Bonetti, and A. E. Williams, "Generalized dual-plane multicoupled line filters," *IEEE Trans. Microwave Theory Tech.*, vol. 41, pp. 2182–2189, Dec. 1993.

[7] H.-C. Chang, C.-C. Yeh, W.-C. Ku, and K.-C. Tao, "A multilayer bandpass filter integrated into RF module board," in *IEEE MTT-S Symp. Dig.*, 1996, pp. 619–622.

[8] J.-S. Hong and M. J. Lancaster, "Couplings of microstrip square open-loop resonators for cross-coupled planar microwave filters," *IEEE Trans. Microwave Theory Tech.* vol. 44, pp. 2099–2109, Nov. 1996.

[9] *EM User's Manual Version 2.4*. Sonnet Software: New York, 1993.

[10] R. Levy, "Filters with single transmission zeros at real or imaginary frequencies," *IEEE Trans. Microwave Theory Tech.* vol. MTT-24, pp. 172–181, Feb. 1976.

Jia-Sheng Hong (M'94) received the D.Phil. degree in engineering science from Oxford University, Oxford, U.K., in 1994.

From 1979 to 1983, he was with Fuzhou University, as a Teaching/Research Assistant in radio engineering. From 1984 to 1985, he was with Karlsruhe University, Germany, where he was involved with microwave and millimeter-wave techniques. In 1986, he returned to Fuzhou University, as a Lecturer in microwave communications. In 1990 he was a graduate member of St. Peter's College, Oxford University, where he conducted research in EM theory and applications. Since 1994, he has been a Research Fellow at Birmingham University, Edgbaston, Birmingham, U.K. His current interests include RF and microwave devices for communications, microwave filters and antennas, microwave applications of high-temperature superconductors, EM modeling, and circuit optimization.

Dr. Hong was awarded a Friedrich Ebert Scholarship and a 1990 K. C. Wong Scholarship presented by Oxford University.

Michael J. Lancaster (M'91) received the physics degree and Ph.D. degree for research into nonlinear underwater acoustics from Bath University, Bath, U.K., in 1980 and 1984, respectively.

He then joined the Surface Acoustic Wave (SAW) Group, Department of Engineering Science, Oxford University, Oxford, U.K., as a Research Fellow, where his research was in the design of new novel SAW devices, including filters and filter banks. These devices worked in the frequency range of 10 MHz–1 GHz. In 1987, he became a Lecturer of EM theory and microwave engineering in the School of Electronic and Electrical Engineering, University of Birmingham, Edgbaston, Birmingham, U.K. Shortly after he joined the University of Birmingham, he began the study of the science and applications of high-temperature superconductors, working mainly at microwave frequencies. He currently heads the Electronic and Materials Devices Group as a Reader. His current personal research interests include microwave filters and antennas, as well as the high-frequency properties and applications of a number of novel and diverse materials.

Dr. Lancaster currently serves on the IEEE Microwave Theory and Techniques Society (MTT-S) International Microwave Symposium Technical Committee.